Journal of Additive Manufacturing Technologies
DOI: 10.18416/JAMTECH.2111539

Infinite Science | Publishing

Investigation of process simulation and additive manufacturability of lattice-type support structures

E. Özeren[1*], B. Pehlivanoğulları[1], C. Şen[1], S. Ören[1], and A. Orhangül[1]

[1] TUSAS Engine Industries Inc., Eskisehir, Turkey
[*] Corresponding author, email: emre.ozeren@tei.com.tr

Abstract

Laser powder bed fusion is an additive manufacturing technology that enables manufacturing complex structures with the capability of design freedom. However, owing to the essential nature of the process, it generally requires support structures. Correct selection of support structures allows a part to be manufactured successfully by avoiding inefficient heat dissipation, process-based failures, redundant material usage and labour-intensive post-processes. For this purpose, alternative support structures to commercial solutions may be needed for manufacturing of the parts. In this study, different lattice-type support structures with nearly same density are investigated in terms of process simulation, manufacturing and inspection. Process simulation results indicate that the simulated lattice-type support structures exhibit similar trend with the actual ones, although up to 35% discrepancy was seen between displacement values which is a result of modelling thin and complex lattice structures. The results from manufacturing show that the lattice-type support structures present more stability than the perforated block-type support structure, although they have the same density. Among the lattice-type support structures, FCC had the minimum deformation in both simulation and manufacturing results. Besides, inspection results show that the manufactured lattice structures have accurate geometrical dimensions which is consistent with its engineering design models.

Keywords: Laser powder bed fusion, lattice structure, support structure, process simulation, additive manufacturing

1. Introduction

In opposition to conventional subtractive methods, in additive manufacturing (AM) technologies parts are produced layer by layer and consume material only needed for the geometry itself [1]. Laser Powder Bed Fusion (L-PBF) is one of the AM technologies in which powder material being melted by laser energy generally in a closed and conditioned building chamber. With the adaptation of engineering materials such as nickel superalloys, aluminium into the AM technologies, L-PBF has started to be widely used in the aerospace industry, which enabled complex and functional component production in less time. Even if the technology promises great advantages to the end-users, there still are some geometric limitations because of the extreme temperature gradients occurred during the process. This physical phenomenon creates excess thermal stresses warping the geometry which may result in a build failure [2]. To minimize manufacturing risks and eliminate geometric limitations, heat dissipated from melt-pool to the build plate has to be managed through supporting structures that increase time and material consumption per part produced [2]. Therefore designing support structures that consume less material and dissipate heat in a more controlled manner is extremely important. Besides, they should be designed in such a way that they can be easily removed from the part after the building process is over.

Manufacturing of lattice structures, which are cellular complex geometries, became also possible with AM technologies. They are being implemented into functional components since even at lower volume fractions they show excellent mechanical resistance to the compressive loads [3], acoustic [5] and vibrational [6] damping capabilities. They also show great heat transfer performance [8-9] due to their extended surface area. Therefore, lattice structures have great potential to be used as a support structure [10]. In literature, different structures were studied as support types Bartsch et al. [3] pointed out topologically optimized support structures to minimize the manufacturing and finishing efforts in L-PBF. The study was combined with L-PBF process simulation technique. Vaidya et al. [11] and Gan et al. [12] focused on creating a sophisticated and advanced support structure to ensure less material usage and good heat dissipation. However, the support creation methods used in these studies require special software solutions and intensive theoretical knowledge. Even though parts with mentioned support structures might have shorter building times, job preparation times might be longer. Since commercial software solutions that offer the creation of lattice structure are getting more accessible, use of lattices as support structure may be an efficient option. Hussein et al. [13] designed two types of skeletal-based Triply Periodic Minimal Surface (TPMS) lattices including its different volume fractions and manufactured the lattices with Ti6Al4V alloy. However, only a small group of lattice structures were examined and deformation analysis was done only on the manufactured parts. It can be concluded that alternative and advanced support structures can be used in order to shorten build time, save material usage and post-process labour time. The novelty of this study is to analyse heat transfer performance of not only TPMS but also strut-based lattice structures with the nearly same density by investigating the process simulation and real displacements. Besides, computer tomography is used for the quality control of the lattice structures. According to the best of the authors' knowledge, there is not any research regarding the computed tomography inspection and manufacturability of Inconel 718 material as lattice-type support structures.

In this study, overhanging L-shaped cantilever beam geometries supported by different types of lattice structures and the shape effects to their heat transfer performances were investigated by releasing the residual stresses through semi-cutting by Wire Electrical Discharge Machining (W-EDM). Building and cutting processes were modelled in a commercial process simulation software. Part displacements were measured with Coordinate Measuring Machine (CMM) and were compared with the simulation results. Additionally geometrical accuracy of the cuboid shape lattice structures was inspected through Computed Tomography (CT).

2. Material and methods

2.1. Lattice-type Support Structure design

Six different lattice-type support structures were designed as shown in Table 1. nTop Platform was used for design and meshing. Lattice types were selected from the family of Triply Periodic Minimal Surface (TPMS) and strut-based which are commonly used and studied in industrial applications and literature. To be able to compare the heat transfer performances of the lattice structures within the identical concept, each lattice structure was designed with nearly the same part volume. In this way, approximately the same amount of material usage for each design was targeted. After that, lattice structures were united with the cantilever beam geometry as given in Fig. 1. Four corner gussets were added to each corner of the cantilever beam as shown Fig 2 to avoid any recoater crash build failure caused by using hard recoater.

Together with the lattice-type support structures, standard block (sB) and perforated block-type support structures as shown in Table 1 were designed. sB support structure was selected as reference and %35 volume reduction of sB was targeted for all other lattice structures and pB to set their the designed volumes to 1,1 cm^3 and the designed porosity to %74. The idea behind of this was to compare lattice-type and perforated block-type support structures in terms of heat transfer performance, deformation behaviour, manufacturability, material usage and job preparation time.

Cuboid samples were also manufactured in the same build plate along with the cantilever beams with lattice and block-type support structures for quality control purposes, as shown in Fig 3. Built lattices were inspected using computed tomography system.

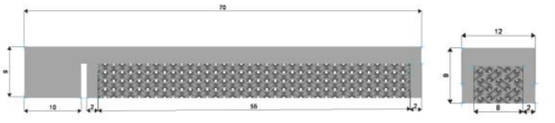

Fig 1. Cantilever beam with lattice structure.

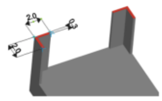

Fig 2. Corner gussets added to cantilever beam.

Table 1. Lattice structures, block-type support and properties.

Lattice Type	**Coding**	**Cell Size**	**Wall Thickness**	**Surface Area**
TPMS Gyroid 	TPMS-G	3x3x3 mm	0.35 mm	8.92 cm^2
TPMS Schwarz 	TPMS-S	3x3x3 mm	0.2 mm	6.84 cm^2
TPMS Diamond 	TPMS-D	3x3x3 mm	0.3 mm	10.94 cm^2
Lattice Type	**Coding**	**Cell Size**	**Strut Diameter**	**Surface Area**
Body Centered Cubic 	BCC	2x2x2 mm	0.5 mm	7.84 cm^2
Face Centered Cubic 	FCC	2x2x2 mm	0.5 mm	9.51 cm^2
Octet-Truss 	OT	3x3x3 mm	0.5 mm	8.79 cm^2
Block Type	**Coding**	**Properties**		
Perforated Block 	pB	**Diamond, beam:** 0,4 mm **Angle:** 60° **Height:** 1mm **Hatching:** 1x1 (x,y) mm **Solid Height:** 0.5 mm		

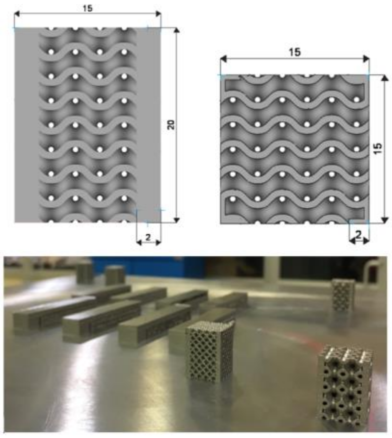

Fig 3. Cuboid samples for quality control purposes.

2.2. Process Simulation

L-PBF process simulations were carried out using MSC Simufact Additive 4.1 software. A thermomechanical model is used in the simulation representing additive manufacturing conditions and process parameters of Inconel 718 material in EOS M400 machine. Parts are placed in the same orientation and position on the build plate as manufactured. Cutting step is added to the simulation after the build step to see the deformations after W-EDM process.

Meshed structure of the geometry is generated through voxel elements in Simufact Additive . Results calculated in those voxel elements are interpolated on the triangular surface mesh to investigate the results on the geometry itself. Since current design tools allow us to generate lattice structures only in stl file format, remeshing tools does not work as good as it works with solid bodies. Sharp corners and the regions where the cantilever beam and lattice cells are connected, are needed to be refined to get more accurate results. Therefore instead of remeshing the geometries, refined surface meshes were generated in nTop platform. 1 mm high precision voxel elements are selected for the parts which is the same as calibration model and 5 mm for the build plate for shorter simulation time.

As an example, surface mesh and voxel mesh of the TPMS-G part is shown in Fig 4.

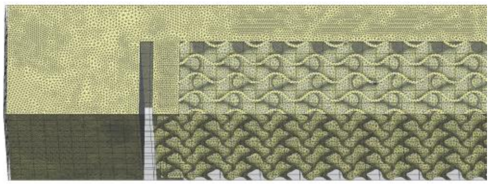

Fig 4. Surface mesh and voxel mesh of TPMS-G.

2.3. Manufacturing, Measurement and Inspection

After design phase completed, build files were prepared with Magics Software. Process parameters and other settings were set in EOSPRINT program. For the lattice-type support structures, 65,7 J/mm^3 volumetric energy density value was used. Job files in single build plate were transferred to the EOS M400 with single yttrium fiber laser L-PBF system for manufacturing. Steel recoater blade was used and non-virgin Inconel 718 powder with spherical morphology and particle size range of 10–63 µm as a feedstock material was processed under argon atmosphere. No heat treatment was performed after L-PBF. The parts were partially cut from 2mm height of build plate surface by Charmilles Cut 300Sp W-EDM machine with a wire of 0.3 mm diameter after AM process as modelled in process simulation phase as shown in Fig. 5.

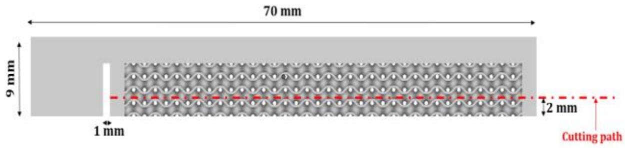

Fig 5. EDM cutting of cantilever beam with TPMS-G.

Laser scanning measurements were done by using LK (Nikon) Altera 15.10.8 CMM 59” x 39” x 31” with LC15Dx following the W-EDM process, in order to evaluate the deformation behaviour and accordingly heat transfer performance. Samples were measured using laser scanner head of the CMM. Since only the displacements were measured, there was no need for the alignment of the parts. Displacements were only measured in build direction, thus only the upper surfaces of the samples were required for the measurement. A point cloud was obtained including the surfaces of samples and the build platform for reference for displacements.

Afterwards, RX-EasyTOM micro CT system was used to investigate geometric dimensions and internal porosity of cuboid lattice structures which were printed together with lattice-type support structures.

3. Results and discussion

3.1. Process Simulation Results

The total displacement distributions along part geometry after several process phases are given in Fig 6. At the end of build and cooling steps displacement result are projected on surface mesh by interpolating the data calculated in voxel elements. On the other hand only voxel mesh results are available after cutting step. TPMS-S geometry is shown in the figure as an example, as the other geometries have similar distribution behaviour. Overall, maximum displacements were found around the same area at the left edge of the parts. The maximum displacement among the lattice structures was seen on TPMS-S, which was found to be 0.26 mm when the last layer of AM process is completed. After the cooling process the maximum displacement was around 0.42 mm, which increased to 1.63 mm in the same area after cutting process. It can be inferred that the deformations were increased after cooling due the residual stresses that occurred in the part and maximized with the deflection of the cantilever beam after cutting.

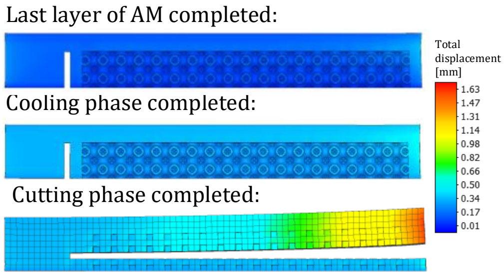

Fig 6. Total displacement distribution of TPMS-S.

3.2. Manufacturing and displacement measurements of parts

Manufacturing of parts with sharp edges and thin walls can be a challenge if a hard recoater is used for L-PBF process, since process based shear forces may occur between blade and the part [14-15]. Recoater crash into thin or sharp edges such as lattice structures with small strut diameter or wall thickness may result in build failures and ultimately cause process to stop.

In this study, despite the fact that no interruption caused by lattice-type support structure was observed, the process was interrupted once because of excessive stresses on the perforated block-type support structure. The structure could not afford stresses of the cantilever beam and deformation on the beam caused recoater crash build failure. This failure was occurred despite of the corner gussets added to the cantilever beam to avoid of any deformation. It can be said that lattice-type support structure could overcome stresses, although pB structure with the same density could not. Failure of the pB structure can be clearly seen in the Fig 7a which illustrates completed build conditions of parts after EDM cut.

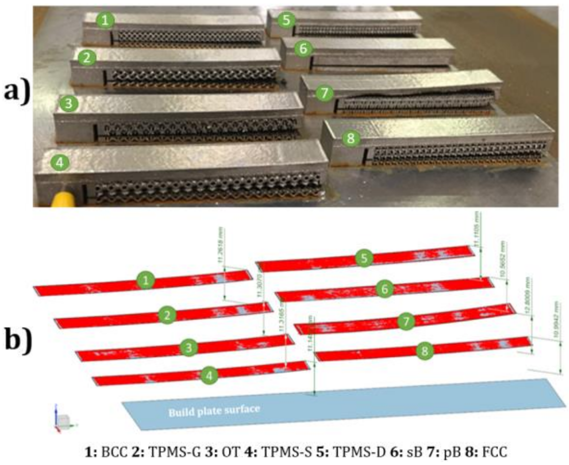

Fig 7. a) Completed build conditions of parts after EDM cut and **b)** laser scanning and displacement measurements.

The point cloud data of laser scanning and displacement measurements in Siemens NX is shown in Fig. 7b. Maximum distances between the surfaces and the reference plane were calculated and compared with the simulation results in Fig. 8. The discrepancy between these two results were up to 35% (except pB, because build failure was seen on this part). The main cause of this discrepancy was insufficient definition of voxel meshing of the thin struts of lattices in the process simulations. Even though the discrepancy between simulation and measurement were high, same trend of both values for different lattice structures were observed.

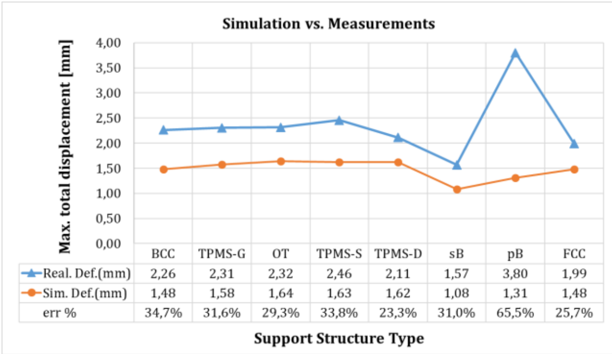

Fig 8. Comparison of deformation values obtained by using measurements and simulations.

It can be seen from the real deformation measurements that there is a distinctive difference between the lattice structures in spite of their lattice families (TPMS or strut-based). For example there is a 0,47 mm maximum displacement between FCC and TMPS-S even though same geometric density is applied. It can be inferred that the heat transfer performance which affects distortions differ with lattice geometry rather than geometric density.

For quality control purposes, CT measurement method was selected due to its ability to measure internal structures and porosity as long as good penetration of X-rays were provided. Geometric measurements of the samples were conducted using wall thickness analyses for practicality. Every strut radius and freeform geometries in TPMS shape were measured simultaneously. In the CT measurements, it was observed that the measurements of all parts were aligned with nominal values within the maximum error of 0.03 mm. Porosity analysis yielded that maximum volumetric porosity in the samples were less than 0.02%. Both measurements proved that the lattice structures could be manufactured with additive method reliably in both geometric and materials sense. An example image of measurement is shown in Fig. 9.

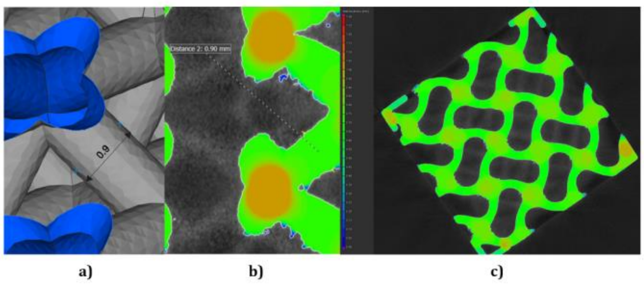

Fig 9. a) Engineering model measurement, **b)** CT measurement of strut diameter of BCC structure and **c)** CT measurement of wall thickness of TPMS-G structure.

4. Conclusions

Lattice-type support structures were investigated in this study with nearly the same density in the aspects of process simulation and manufacturability. The lattice-type support structures presented more stability than the perforated block-type support structure. When taken into account that the material usage and part costs are more important than the other requirements in additive manufacturing of a part, lattice-type support structures may be an option. However, it should not be overlooked that job preparation and laser scanning time for lattice structures are longer than standard supports.

The experimental results showed that among the lattice-type support structures, FCC showed the minimum deformation and TPMS-S showed the maximum deformation. It can be seen that considering TPMS structures which have the same designed volume and cell size, the surface area differs and the bigger surface area causes less deformation. When considering strut-type lattice structures, it can be also seen that a bigger surface area causes less deformation. However, the bigger cell size in OT causes further deformation when comparing with BCC even the surface area of OT is bigger than BCC. It can be concluded that reduced deformation can be achieved via decreasing cell size and increasing surface area.

A similar trend of displacements were observed both in simulations and manufactured parts. However, high numerical discrepancy values were seen when simulation and measurements were compared, which was caused by insufficient representation of the thin struts of lattices by voxel meshing in the process simulations. It was not preferred to conduct further simulations at this time with smaller voxel mesh since the trends were similar and process simulation time increases exponentially with reduced voxel mesh size.

Finally inspection results revealed that each lattice structures were manufactured quite geometrically accurate and with a very small amount of internal porosity.

With the gained knowledge from this research about deformation and heat transfer performance of lattice structures, studies on structural and thermal applications on functional components can be also considered in the future.

Acknowledgments

This study was done with the financial supports of TUSAS Engine Industries Inc.. The authors thank Güray Akbulut for his encouragements.

Author's statement

Conflict of interest: Authors state no conflict of interest. Informed consent: Informed consent has been obtained from all individuals included in this study. Ethical approval: The research related to human use complies with all the relevant national regulations, institutional policies and was performed in accordance with the tenets of the Helsinki Declaration, and has been approved by the authors' institutional review board or equivalent committee.

References

1. Herzog, D., et al., *Additive manufacturing of metals*. Acta Materialia, 2016.
2. Li, C., et al., *Residual Stress in Metal Additive Manufacturing.* Procedia CIRP, 2018. **71**: p.348-353.
3. Bartsch, K., et al., A *Novel Approach to Support Structures Optimized for Heat Dissipation in SLM by Combining Process Simulation with Topology Optimization*. NAFEMS World Congress, 2019. Quebec City, Canada.
4. Maskery, I., Aboulkhair, N. T., Aremu, A. O., Tuck, C. J., & Ashcroft, I. A., *Compressive failure modes and energy absorption in additively manufactured double gyroid lattices*. Additive Manufacturing, 2017. **16**: p. 24-29
5. Wang, X., & Lu, T. J., *Optimized acoustic properties of cellular solids.* The Journal of the Acoustical Society of America, 1999. **106**(2): 756-765.
6. Syam, W. P., Jianwei, W., Zhao, B., Maskery, I., Elmadih, W., & Leach, R., *Design and analysis of strut-based lattice structures for vibration isolation.* Precision Engineering, 2018. **52**:p. 494-506.
7. Wadley, H. N., & Queheillalt, D. T., *Thermal applications of cellular lattice structures.* In Materials science forum, 2007. **539**: p. 242-247.
8. Koneri R., et al., *Additive Manufacturing of Lattice Structures for Heat Transfer Enhancement in Pipe Flow*. Industry 4.0 and Advanced Manufacturing, 2020. p.232-246.
9. Shinomiya, N., et al., *Heat Transfer Performance of Heat Sinks Having Lattice Structure Fabricated Using Metal 3D Printing.* Transactions of the Japan Society of Refrigerating and Air Conditioning Engineers, 2017. **34** (4): p. 435.
10. Saha, K., et al., *Heat Transfer Enhancement and Thermal Performance of Lattice Structures for Internal Cooling of Airfoil Trailing Edges*. J. Thermal Sci. Eng. Appl., 2013. **5**(1): p.9.
11. Vaidya, R. And Anand, S., *Optimum Support Structure Generation for Additive Manufacturing using Unit Cell Structures and Support Removal Constraint*. Procedia Manufacturing, 2016. **5**: p. 1043–1059.
12. Gan, M.X, Wong, C.H., *Practical support structures for selective laser melting*. Journal of Materials Processing Technology, 2016**. 238**: p. 474–484.
13. Hussein, A., et al., *Advanced lattice support structures for metal additive manufacturing*. Journal of Materials Processing Technology, 2013. **213**: p.1019-1026.
14. Dana, M., et al., *The Influence of a Ceramic Recoater Blade on 3D Printing using Direct Metal Laser Sintering, Manufacturing Technology*, 2019. **19**(1): p. 23-28.
15. Bandyopadhyay, A., et al., *Additive Manufacturing,* 2015. CRC Press.